Hindawi
Mathematical Problems in Engineering
Volume 2022, Article ID 8452862, 10 pages
https://doi.org/10.1155/2022/8452862

Research Article

Comparative Analysis of the Effect of Joule Heating and Slip Velocity on Unsteady Squeezing Nanofluid Flow

Hakeem Ullah,[1] **Hina Khan**,[1] **Mehreen Fiza**,[1] **Kashif Ullah**,[1] **Saeed Islam**,[1] **and Seham M. Al-Mekhlafi**[2]

[1]*Department of Mathematics, Abdul Wali Khan University, Mardan, Khyber Pakhtunkhwa, Pakistan*
[2]*Department of Mathematics, Sana'a University, Sanna, Yemen*

Correspondence should be addressed to Mehreen Fiza; drmehreenfiza@gmail.com and Seham M. Al-Mekhlafi; smdk100@gmail.com

Received 14 March 2022; Revised 25 May 2022; Accepted 6 July 2022; Published 16 August 2022

Academic Editor: Arshad Riaz

In this paper, we studied unsteady MHD nanofluid squeezing flow between two parallel plates considering the effect of Joule heating and thermal radiation. The governing equations in the form of partial differential equations (PDEs) are transformed into a system of ordinary differential equations (ODEs) with the help of similarity transformation. The obtained boundary value problem is solved analytically by optimal auxiliary function method (OAFM) and numerically by Runge–Kutta method of order 4 (RKMO4). The OAFM results are validated and compared to the results of RKMO4. The effects of physical parameters such as stretching parameter S, Prandtl number Pr, Eckert number Ec, magnetic number M, volume friction φ electric parameter E_1, and porous parameter γ on the velocity, temperature, and concentration profiles are discussed with the help of plots. Also, the skin friction and Nusselt numbers effects are discussed with the help of tabular data. As the plates move apart, the Nusselt number and the skin friction coefficient decline and the Prandtl number decreases the temperature profile, whereas the stretching and Eckert number increases causing to increase the temperature field.

1. Introduction

A nanofluid is a fluid made up of nanoparticles, which are nanometer-sized particles having diameter less than 100 nm. The concept of nanofluid was given by Choi and Eastman [1]. These fluids are colloidal nanoparticle deferments in a base fluid such as metals, oxides, carbides, and carbon nanotubes are often used as nanoparticles in nanofluids and the base fluids contain water, ethylene glycol, oil, toluene, biofluids, and polymer solution. The nanoparticles are up to 5% of volume fraction in nanofluids. In recent years, many researchers have studied and reported nanofluid technology experimentally or numerically in the presence of heat transfer. The nanofluid have industrial and engineering applications such as electronic cooling devices, chemical factors, heat pumps, and heat exchangers [2–13]. Nanofluid have a variety of features that could make them beneficial in a variety of heat transfer applications. As the heating/cooling fluids have an important role in the energy efficient heat transfer materials. The heat and mass transfer is an important phenomenon in the nanofluid because of its industrial applications such as polymer formation, compression, power transmitting, lubricant system, and food processing. Stephen [14] introduced the idea of squeezing flow under lubrication. Domairry and Hatami studied the flow of squeezed nanofluid between two plates [15]. The unsteady flow of squeezing flow between two parallel plates is studied by Pourmehran et al. [16]. The unsteady squeezed flow is studied by Gupta and Ray [17]. This study has extended by Khan et al. [18] by considering the viscous dissipation properties. Magnetohydrodynamics (MHD) is the effect of magnetic field on the electrical conducting fluid, such as water and [19], which have been presented for the first time. This field have many applications in industry and engineering such as MHD sensors, MHD cooling reactors, and casting. The MHD and heat transfer analysis with thermal radiation of nanofluid is studied by Ibrahim and Shankar [20]. Malvandi and Ganji [21] studied the MHD and heat transfer of nanofluid. The impact of thermal radiation and slip on MHD nanofluid was studied by Haq et al. [22]. Govindaraju et al. [23] studied the entropy analysis of MHD nanofluid. Uddin et al. [24] studied the porous medium of MHD nanofluid flow on the horizontal plate. The stagnation point flow of MHD nanofluid is investigated by Hsaio [25]. The dissipation and chemical reaction analysis for MHD nanofluid is study by Kameswaran et al. [26]. Matin et al. [27] and Pal et al. [28] studied the dissipation analysis and heat transfer analysis over the stretching sheet. The analysis of porous medium on MHD nanofluid flow was studied by Zhang et al. [29]. Elshehbey and Ahmed [30] studied the Buongiorno nanofluid model. The thermal radiation and Ohmic dissipation effects on the MHD flow with heat transfer is studied by Olanreaju [31]. Ullah et al. studied the MHD nanofluid with thermal radiation [32], whereas Rashidi et al. [33] examined the MHD flow caused by heat generation. From the literature, it is shown that the MHD flow over stretching sheets with heat transfer, the effect of electric field, Ohmic dissipation joule, and thermal radiation have not been considered and very little consideration is devoted towards it in the viscous fluids. Having this view, the unsteady MHD nanofluid squeezing flow between two parallel plates considering the effect of Joule heating and thermal radiation is considered. The effect of electric and magnetic fields are considered in the momentum and energy equations, and thermal radiation and Ohmic dissipation are taken into description. The skin friction Nusselt number and Sherwood number are elaborated with the help of tables. The analytical and numerical techniques are used for the treatment of BVP. Normally the numerical techniques require the process of linearization and discretization, which may turn to divergent solutions in some cases. Recently Herisanu [34, 35] presented a new optimal technique OAFM that do not need the linearization/discretization and small parameters issues such as perturbation method. OAFM has a large convergence region, which control the convergence with the help of optimal constant. OAFM provides us the accurate solution at just the first iteration without using the complex mathematical algorithms, and even a low specified computer can run the algorithm easily, and also the procedure of OAFM is very easy in implementation and quick convergent as compared to the other semianalytical methods such as HAM and OHAM. Some recent development in this area can be seen in [37–41].

The objective of this study is to find the analytical (OAFM) and numerical (RKMO4) solutions of unsteady MHD nanofluid squeezing flow considering the effect of Joule heating and thermal radiation. The OAFM results are validated and compared to numerical method results.

2. Basic Ideas of Optimal Auxiliary Functions Method [38, 39]

Assume that the nonlinear differential equation

$$L[\Theta(\eta)] + s(\eta) + \mathrm{N}[\Theta((\eta))] = 0, \tag{1}$$

with the BCs

$$\mathrm{B}\left(\Theta(\eta), \frac{d\Theta(\eta)}{d\eta}\right) = 0. \tag{2}$$

We write the solutions as follows:

$$\Theta(\eta) = \Theta_0(\eta) + \Theta_1(\eta, E_i), \quad i = 1, 2, 3, \ldots\ldots s. \tag{3}$$

The initial approximate solutions is of the following form:

$$L[\Theta_0(\eta)] + s(\eta) = 0, B\left(\Theta_0(\eta), \frac{d\Theta_0(\eta)}{d\eta}\right) = 0. \tag{4}$$

And the first approximation solutions is as follows:

$$\begin{gathered}[\Theta_1(\eta, E_i)] + N[\Theta_0(\eta) + \Theta_1(\eta, E_i)] = 0, \\ B\left(\Theta_1(\eta, E_i), \frac{d\Theta_1(\eta, E_i)}{d\eta}\right) = 0.\end{gathered} \tag{5}$$

Also,

$$\begin{aligned}&N[\Theta_0(\eta) + \Theta_1(\eta, E_i)] \\ &\quad = N[\Theta_0(\eta)] + \sum \frac{d\Theta_1^k(\eta, E_i)}{k} N^k[\Theta_0(\eta)].\end{aligned} \tag{6}$$

The approximated solution is obtained by using equation(3).

The auxiliary functions Eis can be obtained by using the method of least square,

$$J(E_i, E_j) = \int_a^b R^2(m, \lambda, \alpha, \varepsilon) d\varepsilon, \tag{7}$$

where

$$\begin{aligned}R(m, \lambda, \alpha, \varepsilon) = L\left[\Theta(E_i, E_j)\right] + g(\varepsilon) + N\left[\Theta(E_i, E_j)\right], \\ i = 1, 2, \ldots P, j = p+1, p+2 \ldots s.\end{aligned} \tag{8}$$

And

$$\frac{\partial J}{\partial E_1} = \frac{\partial J}{\partial E_2} = \frac{\partial J}{\partial E_3} = \ldots \frac{\partial J}{\partial C_P} = \frac{\partial J}{\partial E_{P+1}} = \ldots \frac{\partial J}{\partial E_s} = 0. \tag{9}$$

3. Problem Formulation and Solution

We consider the unsteady two-dimensional flow of squeezed nanofluid between two parallel plates with heat and mass transfer with water as base fluid and nanoparticles as copper (Cu), silver (Ag), alumina (Al_2O_3), and titanium oxide (TiO_2). A uniform magnetic field is applied vertically to the direction of flow and the plates. The separation of the plates is given as $z = \pm l(1-\alpha t)^{(1/2)} = \pm h(t)$, where l is the initial position (at time $t = 0$). The flow is considered incompressible with no chemical reaction. The fluid is electrically conducting in the presence of applied magnetic field $\overline{B} = (0, B_0, 0)$ and electric field $\overline{E} = (0, 0, -E_0)$. The flow is due to squeezing. The electric and magnetic fields obeys the Ohms law "$\overline{J} = \sigma(\overline{E} + \overline{V} \times \overline{B})$," where $\overline{J}$ is the Joule current, σ is the electrical conduction, and $\overline{E}$ and $\overline{V}$ are electric and velocity fields. The induced magnetic field and Hall current are ignored and the electric and magnetic field contribute in the momentum and thermal heat equation. The flow description can be seen in Figure 1.

The fundamental equations are as follows:

$$\begin{aligned}
&\partial_x u + \partial_y v = 0,\\
&\rho_{nf}\left(\partial_t u + u\partial_x u + v\partial_y u\right)\\
&\quad = -\frac{\partial p}{\partial x} + \mu_{nf}\left(\partial_{xx} u + \partial_{yy} u\right) - \sigma_{nf}\left(E_0 B_0 - B_0^2 u\right),\\
&\rho_{nf}\left(\partial_t v + u\partial_x v + v\partial_y v\right)\\
&\quad = -\frac{\partial p}{\partial y} + \mu_{nf}\left(\partial_{xx} v + \partial_{yy} v\right),\\
&\left(\partial_t T + u\partial_x T + v\partial_y T\right)\\
&\quad = \frac{k_{nf}}{\left(\rho C_p\right)_{nf}}\left(\partial_{xx} T + \partial_{yy} T\right)\\
&\quad + \frac{\mu_{nf}}{\left(\rho C_p\right)_{nf}}\left(4\left(\partial_{xx} u\right)^2 + \left(\partial_y u + \partial_x v\right)^2\right)\\
&\quad + \frac{\sigma_{nf}}{\rho}\left(u B_0 - E_0\right)^2, \textit{ and}\\
&\partial_t C + u\partial_x C + v\partial_y C = D\left(\partial_{xx} C + \partial_{yy} C\right).
\end{aligned} \tag{10}$$

With BCs,

$$\begin{aligned}
&v = \frac{dh}{dt},\\
&u = -L\partial_y u,\\
&C = C_h,\\
&T = T_h,\\
&y = h(t),\\
&v = \partial_y u\\
&\quad = \partial_y T\\
&\quad = 0,\\
&C = C_0,\\
&T = T_0,\\
&y = 0,
\end{aligned} \tag{11}$$

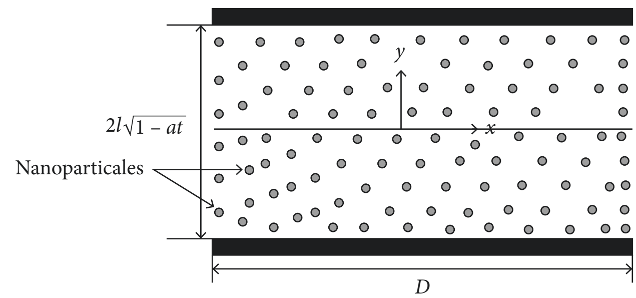

Figure 1: Schematic representation of the problem.

and

$$\begin{aligned}
&\mu_{nf} = \frac{\mu_f}{(1-\phi)^{2.5}} \text{ (Brinkman)},\\
&\frac{K_{nf}}{K_f} = \frac{2K_f + K_s - 2\phi\left(K_f - K_s\right)}{2K_f + K_s + 2\phi\left(K_f - K_s\right)} \text{ (Garnetts Maxwell), } \textit{and}\\
&\sigma_{nf} = (1-\phi)\sigma_f + \phi\sigma_s.
\end{aligned} \tag{12}$$

Using the following similarity variable as [40].

$$\begin{aligned}
&u = \frac{\alpha x}{2(1-\alpha t)} f'(\eta),\\
&\theta = \frac{T - T_0}{T_h - T_0},\\
&\phi = \frac{C - C_0}{C_h - C_0},\\
&\eta = \frac{y}{l(1-\alpha t)^{1/2}}.
\end{aligned} \tag{13}$$

With the help of similarity variable obtain in the above codes,

$$\begin{aligned}
&f'''' - \mathrm{SA}_1 (1-\varphi)^{2.5}\left(f' f'' + 3f'' + \eta f''' - f f'''\right) -\\
&- M^2\left(E_1 - f'\right) = 0, -M^2\left(E_1 - f'\right),
\end{aligned} \tag{14}$$

and

$$\begin{aligned}
&A_1 = (1-\varphi) + \varphi\frac{\rho_S}{\rho_f},\\
&A_2 = (1-\varphi) + \varphi\frac{\left(\rho C_p\right)_s}{\left(\rho C_p\right)_f}, \text{ and}\\
&A_3 = \frac{k_{nf}}{k_f}.
\end{aligned} \tag{15}$$

Here, A1, A2, and A3 are dimensionless constants, $S = ((al2)/(2vf))$ is the squeeze number, $\mathrm{Pr} = \mu f(((pCp)f)/(pfkf))$ is the Prandtl number, $Sc = ((vf)/(Dn\ f))$ is Schmidt number, and

$\delta = ((L)/l(1-\alpha t)^{(1/2)})$ is the velocity slip parameter,$Ec = (pf/((pCp)f))((\alpha\eta)/2(1-\alpha t))^2$ is the Eckert number,$M^2 = ((\sigma B_0^2)/(\rho\alpha))$ is magnetic number, and $E_1 = ((2E_0(1-\alpha t))/(B_0))$ is the electrical number.

The BCs are as follows:

$$\begin{aligned}\theta'(0) &= 0,\\ f''(0) &= 0,\\ f(0) &= 0,\\ \phi(0) &= 0,\\ f(1) &= 1,\\ f'(1) &= -\delta f''(1),\\ \theta(1) &= 1, \text{ and}\\ \phi(1) &= 1.\end{aligned} \tag{16}$$

The physical quantities of interest are the skin-friction coefficient Cf, the Nusselt number Nu_x, and the Sherwood number Sh_x, defined as follows:

$$\begin{aligned}Nu_x &= \frac{Iq_w}{k_f(T_h - T_0)},\\ C_f &= \frac{T_w}{\rho_{nf} v^2 w},\\ Sh_x &= \frac{lm_w}{D(C_h - C_0)},\end{aligned} \tag{17}$$

where $m_w = -D_{nf}\left(\partial_y C\right)_{y=h(t)}$, and

$$T_w = \mu_{nf}\left(\partial_y u\right)_{y=h(t)}.$$

Using the dimensionless form as follows:

$$\begin{aligned}-A_3\theta'(1) &= Nu_x,\\ Sh &= -\phi(1), \text{ and}\\ C_f &= \frac{f''(1)}{A_1(1-\varphi)^{2.5}},\end{aligned} \tag{18}$$

we obtained

$$\begin{aligned}&f^{iv} - \mathrm{SA}_1(1-\varphi)^{2.5}\left(f'f'' + 3f'' + \eta f''' ff'''\right)\\ &\quad - M^2(E_1 - f') = 0,\\ &\theta'' + \mathrm{Pr}S\left(\frac{A_2}{A_3}\right)(\theta' f - \eta\theta') + \frac{EcPr}{A_3(1-\varphi)^{2.5}}\left(f''^2 4\phi^2 + f'^2\right)\\ &\quad + M^2\mathrm{Pr}(f' - E_1)^2 = 0, \textit{ and}\\ &\phi'' + (ScSf\phi' - ScS\eta\phi') = 0.\end{aligned} \tag{19}$$

Boundary conditions are as follows:

$$\begin{aligned}\theta'(0) &= 0,\\ f(0) &= 0,\\ f'(0) &= 0,\\ \phi(0) &= 0,\\ f(1) &= 1,\\ f'(1) &= -\delta f''(1),\\ \theta(1) &= 1, \text{ and}\\ \phi(1) &= 1.\end{aligned} \tag{20}$$

The linear and nonlinear operators are given as follows:

$$\begin{aligned}L(f(\eta)) &= f^{iv}(\eta),\\ L(\theta(\eta)) &= \theta''(\eta),\\ \phi L(\theta(\eta)) &= \phi''(\eta),\\ N(f(\eta)) &= \mathrm{SA}_1(1-\varphi)^{2.5}(f'f'' + 3f''' + \eta f''' - ff''')\\ &\quad - M^2(E_1 - f')\\ &= 0,\\ N(\theta(\eta)) &= \mathrm{Pr}S\left(\frac{A_2}{A_3}\right)(\theta' f - \eta\theta')\\ &\quad + \frac{EcPr}{A_3(1-\varphi)^{2.5}}\left(4\phi^2 f'^2 + f''^2\right) + M^2\mathrm{Pr}(f' - E_1)^2\\ &= 0, \text{ and}\\ N(\phi(\eta)) &= (ScSf\phi' - ScS\eta\phi') = 0.\end{aligned} \tag{21}$$

We have,

$$\begin{aligned}\theta'(0) &= 0,\\ f''(0) &= 0,\\ f(0) &= 0,\\ \phi(0) &= 0,\\ &\text{when } x = 0,\\ f(1) &= 1,\\ f'(1) &= -\delta f'(1),\\ \theta(1) &= 1,\\ \phi(1) &= 1,\\ &\text{when } x = 1,\\ \phi''(\eta) &= 0, \text{ and}\\ \phi(1) &= 1.\end{aligned} \tag{22}$$

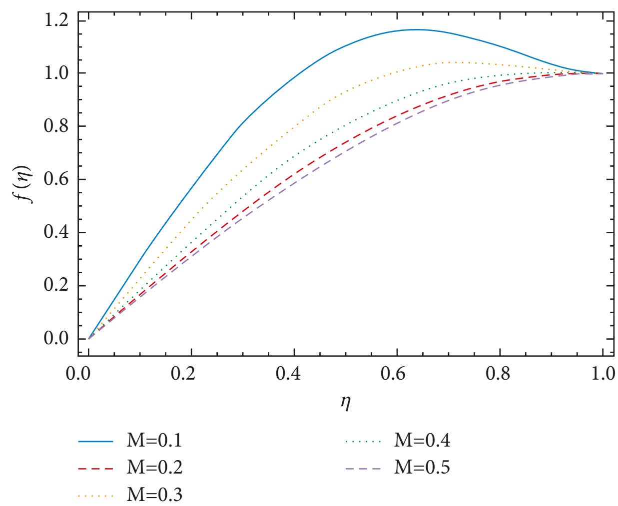

FIGURE 2: M versus $f(\eta)$.

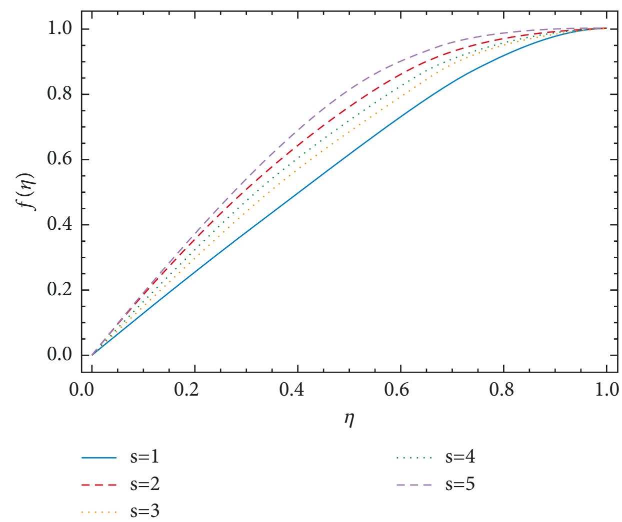

FIGURE 3: S versus $f(\eta)$.

The initial solutions are as follows:

$$\begin{aligned} f(\eta) &= \frac{1}{2}\left(3\eta - \eta^3\right), \\ \theta(\eta) &= \eta^2, \text{ and} \\ \phi(\eta) &= \eta. \end{aligned} \tag{23}$$

Also,

$$\begin{aligned} N(f(\eta)) &= -SA_1(1-\phi)^{2.5} \\ &\quad \left[-3\eta - 9 - 3x\left(\frac{3-x^2}{2}\right) + 3\left(\frac{3x-x^3}{2}\right)\right., \\ N(\theta(\eta)) &= \Pr S\left(\frac{A_2}{A_3}\right)\left[3x^2 - x^4\right] - 2\eta x \\ &\quad + \frac{\Pr Ec}{A_3(1-\varphi)^{2.5}} - 5x^2\left\{\frac{9}{2}\left(1 - x^2 + \frac{1}{2}x^4\right)\right\}, \text{ and} \\ N(\phi(\eta)) &= ScS\left\{\left(\frac{3x-x^3}{2}\right)\right\} - \eta = 0. \end{aligned} \tag{24}$$

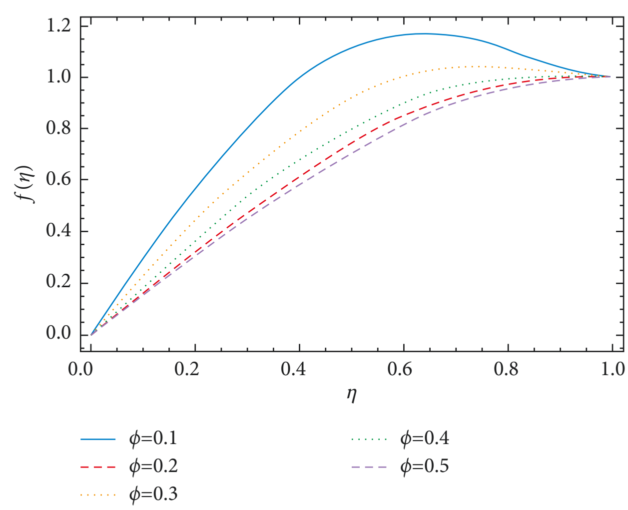

FIGURE 4: φ versus $f(\eta)$.

The first approximation, we have the following equation:

$$\begin{cases} f^{iv}(\eta) + D_1\left(\eta, \eta^2, E_i\right)\left\{\left(-SA_1(1-\phi)^{2.5}\right)\right\}\left[-3\eta - 9x + \left(\frac{3-3x^2}{2}\right)(-3xM) - \left(\frac{3x-x^3}{2}\right)(-3)\right] + 3E_1 x = 0, \\ \theta\prime\prime(\eta) + D_3\left(\eta, \eta^2, E_p\right)\Pr S\left(\frac{A_2}{A_3}\right)\left[3x^2 - x^4\right] - 2\eta x + \frac{\Pr Ec}{A_3(1-\phi)^{2.5}} - 5x^2\left\{\frac{9}{2}\left(1 - x^2 + \frac{1}{2}x^4\right)\right\} + D_4\left(\eta, \eta^2, Em\right) = 0, \\ \phi''(\eta) + D_5\left(\eta, \eta^2, E_r\right)ScS\left(\frac{3x-x^3}{2}\right) - \eta + D_6\left(\eta, \eta^2, En\right) = 0. \end{cases} \tag{25}$$

The OAF can be chosen freely as follows:

$$\begin{cases} D_1(f_0(\eta), E_i) = -(E_1 + E_2\eta), \\ D_2\big(f_0(\eta), E_j\big) = -(E_3 + E_4\eta)e^{-\eta} - \big(E_5 + E_6\eta + E_7\eta^2\big)e^{-2\eta}, \\ D_3(f_0(\eta), E_P) = 0, \\ D_4(f_0(\eta), E_m) = -(E_8 + E_9\eta)e^{-\eta} - \big(E_{10} + E_{11}\eta + E_{12}\eta^2\big)e^{-2\eta}, \\ D_5(f_0(\eta), Er) = -(E_{13} + E_{14}\eta)e^{-\eta} - \big(E_{15} + E_{16}\eta + E_{17}\eta^2\big)e^{-2\eta} \\ D_6(f_0(\eta), E_n) = -(E_{18} + E_{19}\eta)e^{-\eta} - \big(E_{20} + E_{21}\eta + E_{22}\eta^2\big)e^{-2\eta}. \end{cases} \tag{26}$$

We get,

$$\begin{aligned} & f^{iv}(\eta) + D_1\big(\eta, \eta^2, E_i\big)\big\{\big(-SA_1(1-\phi)^{2.5}\big)\big\} \\ & \quad \left[-3\eta - 9x + \left(\frac{3-3x^2}{2}\right)(-3x) - \left(\frac{3x - x^3}{2}\right)(-3)\right] \\ & \quad + 3ME_1x = 0, \\ & \theta''(\eta) + D_3\big(\eta, \eta^2, E_p\big)\Pr S\left(\frac{A_2}{A_3}\right)\left[3x^2 - x^4\right] - 2\eta x \\ & \quad + \frac{\Pr Ec}{A_3(1-\phi)^{2.5}} - 5x^2\left\{\frac{9}{2}\left(1 - x^2 + \frac{1}{2}x^4\right)\right\} \\ & \quad + D_4\big(\eta, \eta^2, Em\big) = 0, \text{ and} \\ & \phi''(\eta) + D_5\big(\eta, \eta^2, E_r\big)ScS\left(\frac{3x - x^3}{2}\right) - \eta \\ & \quad + D_6\big(\eta, \eta^2, En\big) = 0. \end{aligned} \tag{27}$$

The final results is furnished by using the convergence control constants Es.

4. Results and Discussion

4.1. Graphical Discussion. In this section, the results are discussed in detail with the help of graphs. Figure 2 shows the effect of the magnetic and electric fields on the velocity profile. As the magnetic and electric fields increases, the velocity profile decreases. Since the magnetic and electric field oppose the electrically conducting fluid and as a result the velocity of the fluid reduces. Figure 3 shows the effect of stretching parameter s on the velocity field. Growth in the stretching parameter causes the velocity profile to rise. Since the stretching parameter is increased, it assists the flow, and hence the velocity of the fluid is increased. The effect of the volume friction on the velocity profile can be seen in Figure 4. The volume friction reduces the velocity profile and act as opposing force to the flow. The effect of the Prandtl number and volume friction numbers on the temperature profile are observed in Figures 5 and 6. The temperature profile is reduced when increasing the Prandtl and volume friction numbers. Since the Prandtl/volume friction number increase kinetic energy of the particle and the elastic collision of the particles reduces the temperature profile. The effect of stretching parameter and Eckert number are depicted in Figures 7 and 8. The same behavior

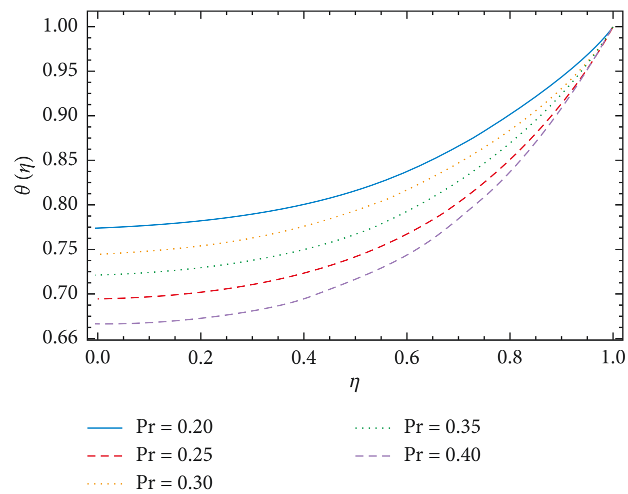

Figure 5: Pr versus $\theta(\eta)$.

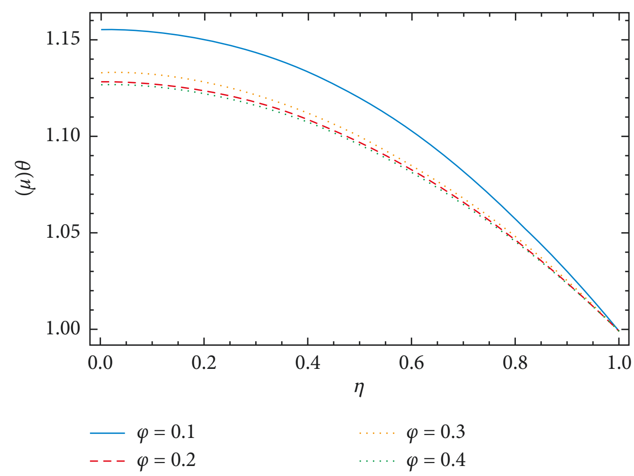

Figure 6: φ versus $\theta(\eta)$.

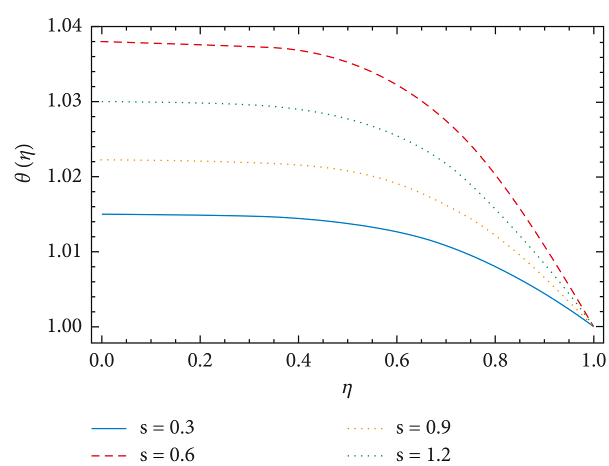

Figure 7: s versus $\theta(\eta)$.

of both the parameter is observed for the temperature profile as it increases the temperature profile. Also the effect of the stretching parameter and Schmidt number on the concentration profile can be seen in Figures 9–11. By increasing the stretching and Schmidt numbers the

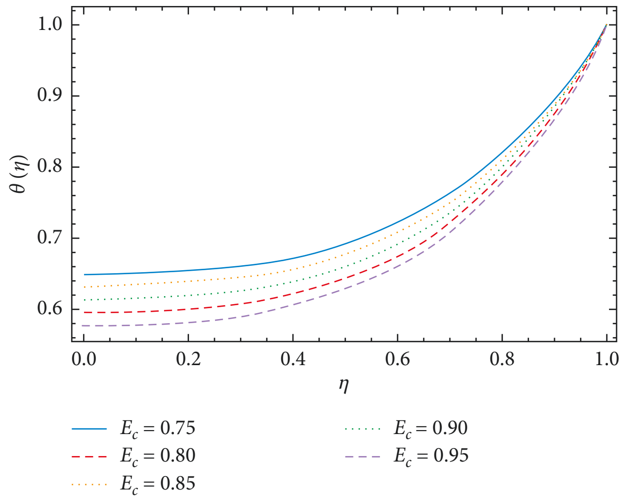

Figure 8: Ec versus $\theta(\eta)$.

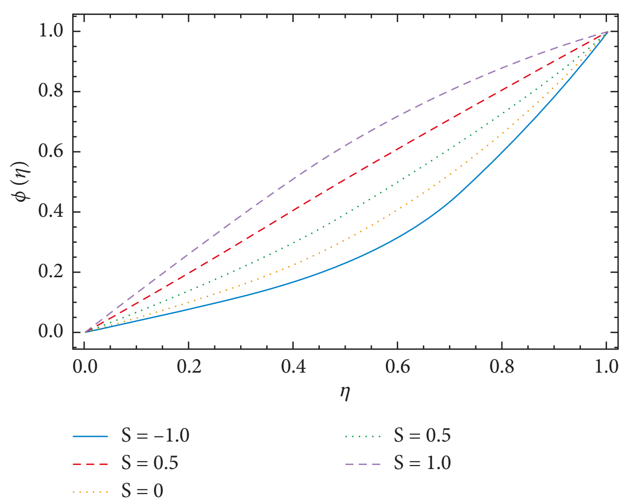

Figure 9: S versus $\theta(\eta)$.

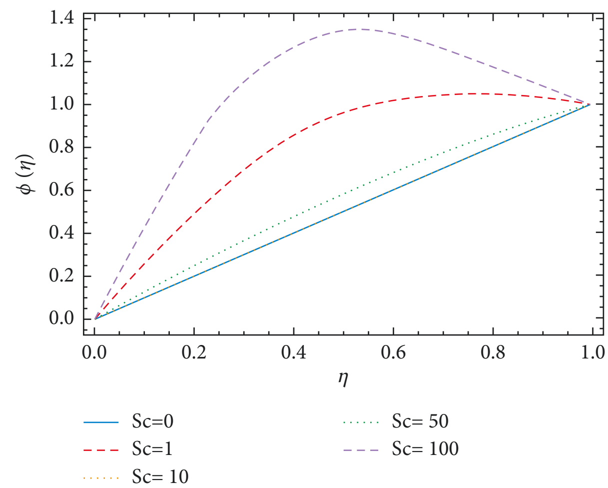

Figure 10: Sc versus $\theta(\eta)$.

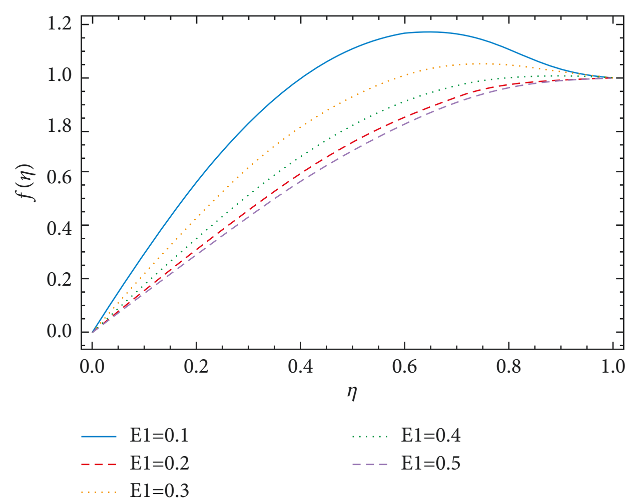

Figure 11: E1 versus $f(\eta)$.

concentration profile increases. Also, the effects of magnetic and electric fields on the temperature profiles are given in Figures 12 and 13. The temperature profile decreases by increasing the magnetic field. It is due to the fact that increasing the magnetic field increases the elastic collision of the nanoparticles, which reduces the temperature profile. We obtain the opposite effect of the electric field on the temperature profile as compared to the magnetic effect on the temperature profile.

4.2. Tables Discussion. The influence of S on the skin-friction coefficient Cf, Nusselt number Nux, and the Sherwood number Sh are tabulated in Table 1. By increasing S, the Cf and Nux decreases while Sh increases. The influence of Ec on Cf, Nux, and Sh are shown in Table 2. By increasing Sc, the Cf, Nux, and Sh decreases. Also the influence of M is tabulated for various values of M on Cf, Nux, and Sh in Table 3. From this table it is clear that by increasing M, Cf reduces while Nux and Sh

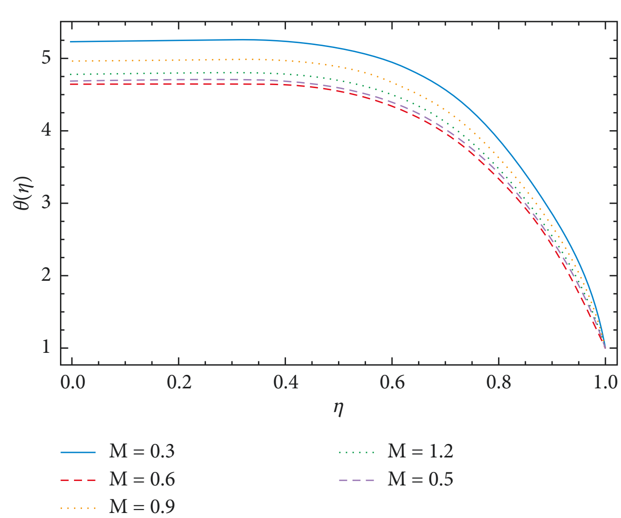

Figure 12: M versus $\theta(\eta)$.

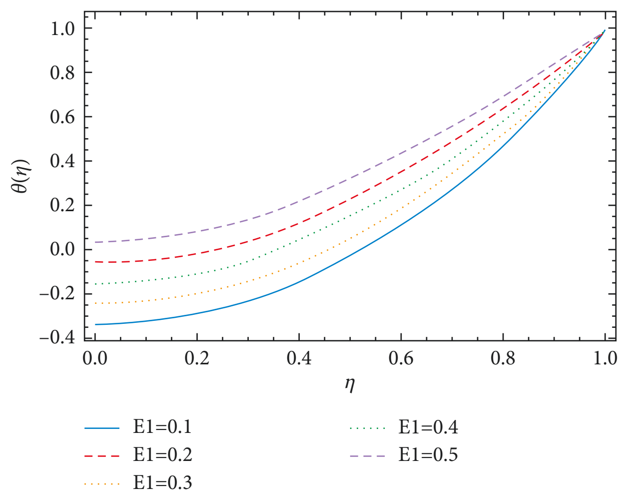

Figure 13: E1 versus $\theta(\eta)$.

Table 1: Impact of S on Cf, Nux, and Sh.

s	C_f	Nu_x	Sh_x
0.1	−2.54526	0.25486	−2.065879
0.2	−1.34295	0.187977	−1.0694254
0.3	−2.09419	0.104693	−1.0000000
0.4	−3.054689	0.054896	−0.987563
0.5	−4.021458	0.0012458	−0.568963

Table 2: Impact of Ec on Cf, Nux, and Sh.

Ec	C_f	Nu_x	Sh_x
0.1	−2.54862	0.025486	−0.56896
0.2	−2.52145	0.087562	−0.56875
0.3	−2.47856	0.082542	−0.58952
0.4	−2.36548	0.081546	−0.487563

Table 3: Impact of M on Cf, Nux, and Sh.

M	C_f	Nu_x	Sh_x
1	−2.854785	0.035689	−0.487596
2	−2.88546	0.087546	−0.487593
3	−2.98563	0.087562	−0.488236
4	−2.845263	0.045785	−0.489596

Table 4: Impact of φ on Cf, Nux, and Sh.

φ	C_f	Nu_x	Sh_x
0.10	−1.02154	0.054256	−0.63256
0.20	−1.021485	0.054120	−0.658523
0.30	−1.021496	0.051243	−0.658745
0.40	−1.21458	0.050852	−0.532110

increases. The effect of nanoparticle volume fraction φ on Cf, Nux, and Sh is presented in Table 4. By increasing φ, Cf increases while Nux and Sh decreases. Again the present method is validated by comparing the results as given in Table 5.

Table 5: Comparison of OAFM and RKMO4 results.

η	$f(\eta)$	$\theta(\eta)$	$f(\eta)$	$\theta(\eta)$
0	0.000000000	0.000000000	0.000000000	0.000000000
0.1	0.14135879	1.14135878	0.14135863	0.14135878
0.2	0.28066639	0.28066638	0.28066669	0.28066638
0.3	0.41578137	0.41578131	0.41578136	0.41578136
0.4	0.54437979	0.54437975	0.54437989	0.54437978
0.5	0.66385837	0.66385835	0.66385852	0.66385836
0.6	0.77123132	0.77123131	0.77123131	0.77123131
0.7	0.86301853	0.86301853	0.86301851	0.86301852
0.8	0.93512364	0.93512365	0.93512362	0.93512362
0.9	0.98270044	0.98270045	0.98270041	0.98270042
1.0	1.00000000	1.00000000	1.00000000	1.00000000

5. Conclusion

The OAFM results are identical to the results obtain from RKMO4 results. OAFM provide us a convenient way to control the convergence in the large flexible region with the help of optimal constants. OAFM contain less computational work and can be easily handle by a low specification computer. The OAFM provides us the first iteration results, which in comparison is proving that the method is simply applicable and provide us the accurate solution even at first iteration.

From the above discussion the following points is of importance.

(i) By increasing S, the Cf and Nux decreases while Sh increases

(ii) By increasing Sc, the Cf, Nux, and Sh decreases.

(iii) By increasing M, Cf reduces while Nux and Sh increases

(iv) By increasing φ, Cf increases while Nux and Sh decreases

(v) Schmidt number increases the concentration profile

(vi) The electrical current resists the flow whereas the stretching parameter assists the flow velocity

(vii) The Prandtl number decreases the temperature profile whereas the stretching and Eckert number increases causes to increase the temperature field

(viii) The stretching and Schmidt numbers increase causes to decrease the concentration profile

(ix) The mention techniques can be applied in future for more complex physical models

Data Availability

All data are available in the paper.

Conflicts of Interest

The authors declare that they have no conflicts of interest.

References

[1] S. U. S. Choi and J. A. Eastman, "Enhancing thermal conductivity of fluids with nanoparticle," in *Proceedings of the International Mechanical Engineering Congress and Exhibition*, pp. 99–105, San Francisco, Calif, USA, November 1995.

[2] M. Azimi and R. Riazi, "Heat transfer analysis of GO-water nanofluid flow between two parallel disks," *Propulsion and Power Research*, vol. 4, no. 1, pp. 23–30, 2015.

[3] M. Fakour, D. D. Ganji, and M. Abbasi, "Scrutiny of underdeveloped nanofluid MHD flow and heat conduction in a channel with porous walls," *Case Studies in Thermal Engineering*, vol. 4, pp. 202–214, 2014.

[4] T. Groşan, C. Revnic, I. Pop, and D. B. Ingham, "Free convection heat transfer in a square cavity filled with a porous medium saturated by a nanofluid," *International Journal of Heat and Mass Transfer*, vol. 87, pp. 36–41, 2015.

[5] A. V. Kuznetsov and D. A. Nield, "The Cheng-Minkowycz problem for natural convective boundary layer flow in a porous medium saturated by a nanofluid: a revised model," *International Journal of Heat and Mass Transfer*, vol. 65, pp. 682–685, 2013.

[6] P. Rana, R. Bhargava, and O. A. Bég, "Numerical solution for mixed convection boundary layer flow of a nanofluid along an inclined plate embedded in a porous medium," *Computers & Mathematics with Applications*, vol. 64, no. 9, pp. 2816–2832, 2012.

[7] A. M. Rashad, A. J. Chamkha, and M. Modather, "Mixed convection boundary-layer flow past a horizontal circular cylinder embedded in a porous medium filled with a nanofluid under convective boundary condition," *Computers & Fluids*, vol. 86, pp. 380–388, 2013.

[8] N. Vishnu Ganesh, B. Ganga, and A. K. Abdul Hakeem, "Lie symmetry group analysis of magnetic field effects on free convective flow of a nanofluid over a semi-infinite stretching sheet," *Journal of the Egyptian Mathematical Society*, vol. 22, no. 2, pp. 304–310, 2014.

[9] Y. Lin, L. Zheng, and G. Chen, "Unsteady flow and heat transfer of pseudo-plastic nanoliquid in a finite thin film on a stretching surface with variable thermal conductivity and viscous dissipation," *Powder Technology*, vol. 274, pp. 324–332, 2015.

[10] M. Sheikholeslami, M. M. Rashidi, and D. D. Ganji, "Numerical investigation of magnetic nanofluid forced convective heat transfer in existence of variable magnetic field using two phase model," *Journal of Molecular Liquids*, vol. 212, pp. 117–126, 2015.

[11] T. Hayat, M. Waqas, S. A. Shehzad, and A. Alsaedi, "Mixed convection flow of a Burgers nanofluid in the presence of stratifications and heat generation/absorption," *The European Physical Journal Plus*, vol. 131, no. 8, p. 253, 2016.

[12] F. M. Abbasi, T. Hayat, S. A. Shehzad, F. Alsaadi, and N. Altoaibi, "Hydromagnetic peristaltic transport of copper-water nanofluid with temperature-dependent effective viscosity," *Particuology*, vol. 27, pp. 133–140, 2016.

[13] M. Sheikholeslami, D. D. Ganji, and M. M. Rashidi, "Magnetic field effect on unsteady nanofluid flow and heat transfer using Buongiorno model," *Journal of Magnetism and Magnetic Materials*, vol. 416, pp. 164–173, 2016.

[14] M. J. Stefan, "Versuchs Uber die scheinbare adhesion, Sitzungs berichte der Akademie der Wissenschaften in Wien," *MathematikNaturwissen*, vol. 69, pp. 713–721, 1874.

[15] G. Domairry and M. Hatami, "Squeezing Cu-water nanofluid flow analysis between parallel plates by DTM-Padé Method," *Journal of Molecular Liquids*, vol. 193, pp. 37–44, 2014.

[16] O. Pourmehran, M. Rahimi-Gorji, M. Gorji-Bandpy, and D. D. Ganji, "RETRACTED: analytical investigation of squeezing unsteady nanofluid flow between parallel plates by LSM and CM," *Alexandria Engineering Journal*, vol. 54, no. 1, pp. 17–26, 2015.

[17] A. K. Gupta and S. Saha Ray, "Numerical treatment for investigation of squeezing unsteady nanofluid flow between two parallel plates," *Powder Technology*, vol. 279, pp. 282–289, 2015.

[18] U. Khan, N. Ahmed, M. Asadullah, and S. Tauseef Mohyud-din, "Effects of viscous dissipation and slip velocity on two-dimensional and axisymmetric squeezing flow of Cu-water and Cu-kerosene nanofluids," *Propulsion and Power Research*, vol. 4, no. 1, pp. 40–49, 2015.

[19] H. Alfvén, "Existence of electromagnetic-hydrodynamic waves," *Nature*, vol. 150, no. 3805, pp. 405-406, 1942.

[20] W. Ibrahim and B. Shankar, "MHD boundary layer flow and heat transfer of a nanofluid past a permeable stretching sheet with velocity, thermal and solutal slip boundary conditions," *Computers & Fluids*, vol. 75, pp. 1–10, 2013.

[21] A. Malvandi and D. D. Ganji, "Brownian motion and thermophoresis effects on slip flow of alumina/water nanofluid inside a circular microchannel in the presence of a magnetic field," *International Journal of Thermal Sciences*, vol. 84, pp. 196–206, 2014.

[22] R. Ul Haq, S. Nadeem, Z. Hayat Khan, and N. Sher Akbar, "Thermal radiation and slip effects on MHD stagnation point flow of nanofluid over a stretching sheet," *Physica E: Low-Dimensional Systems and Nanostructures*, vol. 65, pp. 17–23, 2015.

[23] M. Govindaraju, S. Saranya, A. A. Hakeem, R. Jayaprakash, and B. Ganga, "Analysis of slip MHD nanofluid flow on entropy generation in a stretching sheet," *Procedia Engineering*, vol. 127, pp. 501–507, 2015.

[24] M. J. Uddin, M. N. Kabir, and O. A. Bég, "Computational investigation of Stefan blowing and multiple-slip effects on buoyancy-driven bioconvection nanofluid flow with microorganisms," *International Journal of Heat and Mass Transfer*, vol. 95, pp. 116–130, 2016.

[25] K.-L. Hsiao, "Stagnation electrical MHD nanofluid mixed convection with slip boundary on a stretching sheet," *Applied Thermal Engineering*, vol. 98, pp. 850–861, 2016.

[26] P. K. Kameswaran, M. Narayana, P. Sibanda, and P. V. S. N. Murthy, "Hydromagnetic nanofluid flow due to a stretching or shrinking sheet with viscous dissipation and chemical reaction effects," *International Journal of Heat and Mass Transfer*, vol. 55, no. 25-26, pp. 7587–7595, 2012.

[27] M. H. Matin and I. Pop, "Forced convection heat and mass transfer flow of a nanofluid through a porous channel with a first order chemical reaction on the wall," *International Communications in Heat and Mass Transfer*, vol. 46, pp. 134–141, 2013.

[28] D. Pal and G. Mandal, "Influence of thermal radiation on mixed convection heat and mass transfer stagnation-point flow in nanofluids over stretching/shrinking sheet in a porous medium with chemical reaction," *Nuclear Engineering and Design*, vol. 273, pp. 644–652, 2014.

[29] C. Zhang, L. Zheng, X. Zhang, and G. Chen, "MHD flow and radiation heat transfer of nanofluids in porous media with variable surface heat flux and chemical reaction," *Applied Mathematical Modelling*, vol. 39, no. 1, pp. 165–181, 2015.

[30] H. M. Elshehabey and S. E. Ahmed, "MHD mixed convection in a lid-driven cavity filled by a nanofluid with sinusoidal temperature distribution on the both vertical walls using Buongiorno's nanofluid model," *International Journal of Heat and Mass Transfer*, vol. 88, pp. 181–202, 2015.

[31] P. O. Olanrewaju, "Effects of internal heat generation on hydromagnetic non-Darcy flow and heat transfer over a stretching sheet in the presence of thermal radiation and ohmic dissipation," *World Applied Sciences Journal*, vol. 16, pp. 37–45, 2012.

[32] H. Ullah, M. A. Khan, M. Fiza, K. Ullah, M. Ayaz, and M Seham, "Analytical and numerical analysis of the squeezed unsteady MHD nanofluid flow in the presence of thermal radiation," *Journal of nanomaterial*, vol. 2022, Article ID 1668206, 14 pages, 2022.

[33] M. M. Rashidi, S. Abelman, and N. F. Freidooni Mehr, "Entropy generation in steady MHD flow due to a rotating porous disk in a nanofluid," *International Journal of Heat and Mass Transfer*, vol. 62, pp. 515–525, 2013.

[34] R. Ellahi and A. Riaz, "Analytical solutions for MHD flow in a third-grade fluid with variable viscosity," *Mathematical and Computer Modelling*, vol. 52, no. 9-10, pp. 1783–1793, 2010.

[35] A. Riaz, A. Zeeshan, and M. M. Bhati, "Entropy analysis of a three dimensional wavy flowof erying powell nanofluid," *Math.Prob.Eng.*vol. 2021, Article ID 6672158, 14 pages, 2022.

[36] A. Riaz, A. Razaq, and A. U. Awan, "Magnetic field and permeability effects on Jeffrey fluid in eccentric tubes having flexible porous boundaries," *Journal of Magnetics*, vol. 22, no. 4, pp. 642–648, 2017.

[37] A. Zeeshan, N. Ijaz, A. Riaz, A. B. Mann, and A. Hobiny, "Flow of nonspherical nanoparticles in electro-magnetohydrodynamics of nanofluids through a porous medium between eccentric cylinders," *Journal of Porous Media*, vol. 23, no. 12, pp. 1201–1212, 2020.

[38] N. Herisanu and V. Marinca, "An efficient analytical approach to investigate the dynamics of a misaligned multirotor system," *Mathematics*, vol. 8, no. 7, p. 1083, 2020.

[39] N. Herisanu, V. Marinca, G. Madescu, and F. Dragan, "Dynamic response of a permanent magnet synchronous generator to a wind gust," *Energies*, vol. 12, no. 5, p. 915, 2019.

[40] K. Singh, S. K. Rawat, and M. Kumar, "Heat and mass transfer on squeezing unsteady MHD nanofluid flow between parallel plates with slip velocity effect," *Journal of Nanoscience*, vol. 2016, Article ID 9708562, 11 pages, 2016.

[41] M. Sheikholeslami and D. D. Ganji, "Nanofluid flow and heat transfer between parallel plates considering Brownian motion using DTM," *Computer Methods in Applied Mechanics and Engineering*, vol. 283, pp. 651–663, 2015.